Biosensors and Bioelectronics 177 (2021) 112975

Contents lists available at ScienceDirect

Biosensors and Bioelectronics

journal homepage: http://www.elsevier.com/locate/bios

A naked-eye readout self-powered electrochemical biosensor toward indoor formaldehyde: On-site detection and exposure risk warning

Xiaoxuan Sun [a,b], He Zhang [a,b], Liang Huang [a,b], Shuai Hao [a,b], Junfeng Zhai [a,**], Shaojun Dong [a,b,*]

[a] State Key Laboratory of Electroanalytical Chemistry, Changchun Institute of Applied Chemistry, Chinese Academy of Sciences, Changchun, 130022, China
[b] University of Science and Technology of China, Hefei, 230026, China

ARTICLE INFO

Keywords:
Self-powered biosensor
Gaseous formaldehyde monitoring
Colorimetric sensing
Photolithographic technique
Gel electrolyte

ABSTRACT

The determination of indoor formaldehyde is of great importance to protect individuals against its well-known adverse impact on health. Here, we report on a design of a naked-eye readout self-powered electrochemical biosensor (SPEB) toward gaseous formaldehyde based on the efficient catalytic activity of the formaldehyde dehydrogenase/poly (methylene green)/buckypaper bioanode and the excellent electrochromic property of the Prussian blue (PB) cathode. The SPEB has a planar configuration and is covered with poly(vinyl alcohol) (PVA) as gel electrolyte to provide an inner lateral resistance large enough to enable the progressive discoloration of the patterned PB at cathode, which in turn, making the determination of gaseous formaldehyde feasible by measuring the distance consumed after 10-min exposure. The use of PVA gel electrolyte can also facilitate the observation of the color change due to its excellent transparency. The SPEB shows obvious responses to gaseous formaldehyde in a broad concentration range of 80 and 3000 ppb, covering the important permissible limits of indoor formaldehyde related to human health. The SPEB also exhibits satisfactory results in sensing gaseous formaldehyde released from the real plywood that is one of the dominating sources of the gaseous indoor formaldehyde. The results shown here demonstrate the good potential of the naked-eye readout SPEB as a fast, reliable, and portable tool for on-site determination of gaseous formaldehyde, with the appealing characteristics such as ease of operation, simplicity of configuration, and no requirement of external power sources.

1. Introduction

Formaldehyde is a ubiquitous air pollutant in human living environment (Castner et al., 2018; Chung et al., 2013). Awareness of its seriously diverse health impact has induced a hot demand for on-site determination of formaldehyde in surrounding air and consequently assessment of personal exposure risk (Maddalena et al., 2009; Salthammer et al., 2010; Tang et al., 2009). Since they have no requirement of expensive equipment and professional knowledge, formaldehyde sensors are superior over conventional approaches such as chromatography and fluorescence spectrometry in the field of on-site application. Formaldehyde sensors with different response mechanisms have been proposed (Lin et al., 2011; Suzuki et al., 2003; Wei et al., 2017). Among them, electrochemical formaldehyde biosensors using formaldehyde dehydrogenase (FDH) as an efficient bio-recognition element have attracted special attention due to the appealing characteristics such as the high specificity and sensitivity to formaldehyde, the low operating temperature and no humidity interference (Achmann et al. 2008a, 2008b; Demkiv et al., 2008; Hämmerle et al., 1996). Potentiometric and amperometric techniques have been adopted in previous electrochemical formaldehyde biosensors, leading to the requirement of inbuilt electronic components to trigger electrode reactions, collect signals, and display results. However, the deployment of electronic components is actually at the expense of cost, and poses the shortcomings such as the structural complexity and the need for external power sources. Therefore, development of new electrochemical formaldehyde biosensors is urgently desired to meet the hot demand for on-site formaldehyde determination and consequently individual exposure risk assessment.

* Corresponding author. State Key Laboratory of Electroanalytical Chemistry, Changchun Institute of Applied Chemistry, Chinese Academy of Sciences, Changchun 130022, China.
** Corresponding author. State Key Laboratory of Electroanalytical Chemistry, Changchun Institute of Applied Chemistry, Chinese Academy of Sciences, Changchun 130022, China.
E-mail addresses: jfzhai@ciac.ac.cn (J. Zhai), dongsj@ciac.ac.cn (S. Dong).

https://doi.org/10.1016/j.bios.2021.112975
Received 19 September 2020; Received in revised form 31 December 2020; Accepted 2 January 2021
Available online 6 January 2021

There is a growing interest in self-powered electrochemical biosensors (SPEBs) based on enzymatic biofuel cells (EBFCs) because they have a simple two-electrode configuration and can translate biorecognition events into electric signals spontaneously (Fu et al., 2018; Gai et al., 2017; Hao et al., 2020). Successful determination of various analytes including heavy metal ions and biomolecules has been achieved by using appropriately designed SPEBs in the last two decades (Hou et al., 2015; Wen et al., 2011; Zhou 2015), their practical applications especially for on-site detection, however, have been hampered by the requirement of electronic designs for data collection and display (Aller Pellitero et al., 2017). An amazing alternative solution to this problem is the combination of SPEBs and electrochromic displays (Zhang et al., 2016; Zloczewska et al., 2014). Electrochromic displays can change their color when a current is applied (Celiesiute et al., 2019; Yang et al., 2016). This property enables them to convert the electronic signals of SPEBs to optical form and the change in the color is dependent on the concentration of analytes (Liana et al., 2015). Involvement of electrochromic displays in SPEBs would thus make the SPEBs feasible as colorimetric sensors and, in consequence, sensing information can be readily extracted via naked eye. Further use of smartphones as optical readers can make the colorimetric SPEBs available for quantitative detection (Coleman et al., 2019; Dong et al., 2017). Because of the naked-eye detectable color change and the wide availability of smartphones and Apps, there is no need to integrate electronic parts along with the colorimetric SPEBs. Therefore, the colorimetric SPEBs hold good promise in practical applications. However, despite the obvious advantages of such colorimetric SPEBs, only few successful examples have been reported (Aller Pellitero et al., 2020). More successful examples are thus expected, not only proving their promise in practical applications in different fields, but also revealing the links between sensing performance and factors such as operation modes, electrode materials, sensor configurations, and electrolytes.

In our previous work, we presented a self-powered colorimetric biosensor with satisfactory performance for formaldehyde sensing in aqueous phase (Sun et al., 2019). However, it shows deficiency in terms of rapid and on-site detection of gaseous formaldehyde, mainly attributed to the requirement of sampling and narrow detection range (0.01–0.35 mM, corresponding to 3–112 ppb gaseous formaldehyde at room temperature) (Dong and Dasgupta 1986). In this work, we proposed a prominent naked-eye readout SPEB on a patterned conductive indium tin oxide (ITO) glass substrate toward gaseous formaldehyde, which takes an EBFC as the original prototype, composed of a FDH/poly (methylene green) (PMG)/buckypaper (BP) bioanode and a Prussian blue (PB) cathode (Fig. 1). The planar configuration of the SPEB and the large lateral resistance of the poly (vinyl alcohol) (PVA) gel electrolyte enable the progressive discoloration of the PB cathode in the presence of gaseous formaldehyde. The color front moves far away from the bioanode with the increase of the concentration of gaseous formaldehyde from 80 to 3000 ppb, and the distance between the color front and the bioanode obtained after 10-min gaseous formaldehyde exposure is linear dependence on the concentration of gaseous formaldehyde in a range of 80 and 400 ppb. The SPEBs also exhibit high selectivity to formaldehyde in the presence of potential interference such as acetaldehyde and benzaldehyde. As a proof-of-concept practical application, the SPEBs show satisfying results in determination of the gaseous formaldehyde released from the real plywood samples.

2. Experimental

The details of reagents, materials, and instruments are available in the Supplementary Information.

2.1. Preparation of the naked-eye readout SPEB

The preparation procedure of the SPEB was schematically illustrated in Fig. S1. In brief, an ITO substrate with specific pattern (Fig. S2) was firstly cleaned by sequentially washing with acetone, ethanol, and water under sonication for a few minutes, and dried in nitrogen. Then PB film was deposited electrochemically on the ITO substrate by passing through a constant current in a freshly prepared solution containing 0.50 M potassium chloride (KCl), 0.1 M hydrochloric acid, 2.5 mM potassium ferricyanide (III), and 2.5 mM ferric chloride. The current was firstly held at 40 μA cm^{-2} for 50 s as a preconditioning step and then switched to 40 μA cm^{-2} for PB deposition. The deposition times of 80, 100, and 120 s were used to adjust the amount of PB deposited. PB films were further activated by cycling the potential between 0.4 and 0 V for 2 cycles at a scan rate of 5 mV s^{-1} in a 0.1 M phosphate buffer solution (PBS, pH = 5.5) containing 0.1 M KCl (Itaya and Uchida 1986). The bioanode was attached to the rectangular region of the ITO substrate by means of carbon conductive tape, and then covered by a piece of pre-prepared agar membrane with a through-hole (d = 10 mm). 300 μL PVA gel electrolyte was dropped on the surface of the PB cathode and form a membrane contacting with the agar membrane. The SPEB was disconnected unless 250 μL 0.1 M PBS (pH = 7.8) containing 5 mM nicotinamide adenine dinucleotide (NAD^+) was added (Fig. S3).

2.2. Gaseous formaldehyde detection

A modified desiccator method of the European Standard (ISO/CD 12460–4:2016) was used for measuring gaseous formaldehyde (Fu and Zhang 2018). In brief, A cylindrical container with a volume of 880 mL (diameter = 10.6 cm, height = 10.0 cm) was used as the desiccator. A SPEB was placed in the middle of the container and connected with an electrochemical workstation through conductive tapes when electrochemical measurements were performed. The container was lidded to get excellent airtightness. A small volume of supporting electrolyte (250 μL 0.1 M PBS containing 5 mM NAD^+, pH = 7.8) was dropped at the bioanode through a little hole for measuring. The hole could be opened

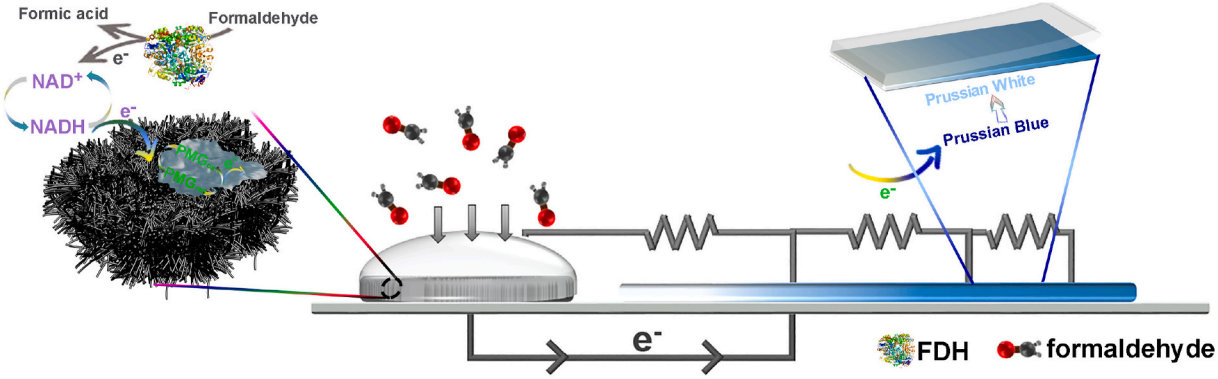

Fig. 1. Working principle of the naked-eye readout SPEB.

and closed manually. The standard gaseous formaldehyde was obtained with a series of formaldehyde solutions and the equilibrium concentrations of gaseous formaldehyde at 37 °C were calculated according to previous work (Zhou and Mopper 1990).

For the real sample test, four pieces of plywood samples (60 mm × 30 mm) were put inside the container and supported by a metal stand. The sides of the plywood were sealed with tapes and the total exposed surface area was 144 cm^2. After 50 min at 23 ± 2 °C (50% ± 10% relative humidity), the container was transferred to 37 °C for formaldehyde detection with the SPEB. The formaldehyde biosensor reported in our previous work was also employed to determine the gaseous formaldehyde emitted from the plywood samples (Sun et al., 2019). In order to get a liquid sample, a watch glass (d = 5.0 cm) containing 24 mL water was placed at the bottom of the container to adsorb gaseous formaldehyde. After 24 h, the water was mixed with 0.2 M PBS (pH = 6.0) of equal volume and transferred to 37 °C, and the concentration of formaldehyde was detected with the biosensor reported previously according to the standard addition method. The standard formaldehyde samples with concentrations of 0.01 mM, 0.02 mM, and 0.03 mM were added for 4 times, respectively.

3. Results and discussion

3.1. Characterization of the FDH/PMG/BP bioanode

The bioanode was prepared by depositing PMG and FDH on the conductive BP substrate in sequence (Sun et al., 2019). The use of BP as the substrate can be mainly attributed to their appealing properties like large specific surface areas, good biocompatibility, and high conductivity besides commercial availability (Gross et al., 2018). The biorecognition event of formaldehyde leads to the reduction of NAD^+ to hydrogenated nicotinamide adenine dinucleotide (NADH) when using FDH as the sensing element (Roche et al., 2014), the sensing information can thus be transduced into electronic signals by oxidation of NADH to NAD^+ at electrodes. However, the potential for NADH oxidation at BP electrode is too high to meet the criteria for constructing SPEB with PB cathode. PMG has proven their ability to shuttle electrons between NADH and electrodes at a relatively low potential (Narváez Villarrubia et al., 2011), so PMG is adopted as an appropriate mediator in this work, aiming at making the bioanode feasible for constructing a SPEB with PB cathode.

BP electrodes are composed of randomly oriented nanotubes and possess porous structure, and the pores are filled with precipitates after electrochemical exposure to methylene green monomer, demonstrating the successful deposition of PMG through the electrochemical approach, as shown in Fig. 2A. A certain amount of FDH solution was dropped on the PMG/BP electrodes and then the FDH/PMG/BP bioanodes could be obtained. Fig. 2B represents the amperometric behaviors of a bioanode in the presence and absence of formaldehyde. Because of the excellent catalytic activity of PMG, the bioanode enables the NADH oxidation to occur at the potential as low as −0.22 V and offer an oxidation peak located at −0.10 V. When feeding with 2 mM formaldehyde, the peak current increases from 0.33 mA cm^{-2} to 0.49 mA cm^{-2} due to the interconversion of NAD^+/NADH between FDH and electrodes. The increased peak current intensity suggests the biological activity of FDH is retained, despite the confinement on electrode surfaces. Moreover, the peak potential for NADH oxidation at the bioanode is much lower than that for PB reduction, thus the construction of a colorimetric SPEB by coupling the bioande and a PB cathode is possible in theory.

The bioanodes with different loading amounts of FDH have also been

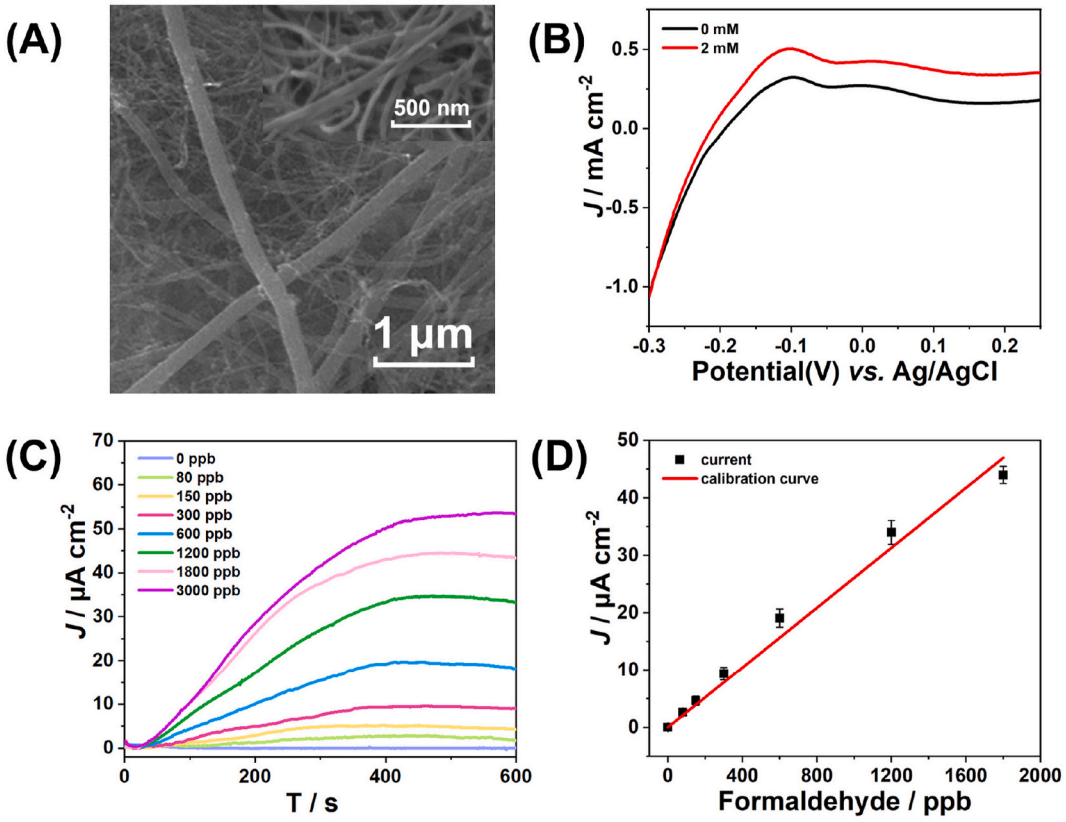

Fig. 2. (A) Scanning electron microscope (SEM) image of the PMG/BP electrode (inset: BP electrode without PMG deposition). (B) Linear sweep voltammograms of the FDH/PMG/BP bioanode in the absence and presence of 2 mM formaldehyde at a scan rate of 5 mV s^{-1}. (C) Chronoamperometric response of the FDH/PMG/BP bioanode towards different gaseous formaldehyde concentrations in the range of 80–3000 ppb. (D) Plot of the value of current at 500 s in Fig. 2C versus the concentration of gaseous formaldehyde. Error bars: standard deviations, n = 3.

prepared by varying the FDH solution concentrations, and their amperometric responses to gaseous formaldehyde with a concentration of 1800 ppb were investigated by recording the current at 0 V. 250 μL PBS containing 5 mM NAD^+ was dropped on the bioanode and used as the electrolyte solution. When the concentrations of the FDH solutions increasing from 0.5 mg mL^{-1} to 2.0 mg mL^{-1}, a gradual increase of the current densities from 28.1 μA cm^{-2} to 43.2 μA cm^{-2} can be observed (Fig. S4), demonstrating the important role of the loading amount of FDH in determining the amperometric response of the bioanode to formaldehyde. Since further increasing the concentration of FDH solutions can hardly lead to the increase of the current densities, the concentration of FDH solution is optimized to be 2.0 mg mL^{-1}, to not only avoid the adverse impact of insufficient FDH amount on the sensing performance such as narrowed dynamic range and low sensitivity, but also provide large current to drive the electrochromic PB cathode. The bioanodes prepared with 2.0 mg mL^{-1} FDH were used for the following experiments.

The chronoamperometric curves at a bioanode were further collected at 0 V under different concentrations of gaseous formaldehyde. 250 μL PBS containing 5 mM NAD^+ was dropped at the bioanode to support both electrochemical and biological reactions occurring at the bioanode. The currents increase immediately after exposure to gaseous formaldehyde owing to the small volume of the electrolyte solution, as shown in Fig. 2C. The higher concentration of gaseous formaldehyde results in the longer time required for the current to reach steady states. The values of the steady-state currents obtained at 500 s are proportional to the concentration of gaseous formaldehyde in the range from 80 to 1800 ppb (Fig. 2D), suggesting the output of the bioanode is formaldehyde-diffusion limited in such a broad concentration range.

3.2. Characterization of the PB cathode

PB cathodes were prepared by electrochemically depositing PB on patterned ITO electrodes and the electrochemical deposition of PB was achieved at a constant current of −40 μA cm^{-2}. As an example, the polarization curve for PB deposition with a deposition time of 100 s is shown in Fig. 3A. The patterned ITO electrode is preconditioned at a constant current of 40 μA cm^{-2} for 50 s, and then the applied current switches to −40 μA cm^{-2} for PB deposition. During the PB deposition, the potential gradually decreases from 0.6 to 0.4 V, dominated by the concentration polarization. Despite the decrease, the potential is still higher than that for ferricyanide reduction, confirming that the deposition of PB is attributed to the electrochemical reduction of Fe^{3+} but not ferricyanide. A SEM image shown as the inset in Fig. 3B reveals that the electrochemically deposited PB has a dense granular structure with obvious cracks. After activation, a uniform PB film without cracks can be obtained, the disappearance of the cracks can be mainly ascribed to the exchanges of potassium ions between PB crystal structure and the activation solution (Itaya and Uchida 1986). At the PB cathode, there are micron-sized round holes with uniform distribution (Fig. S5). Compared with the PB electrode without micropores, the peak potential difference obtained from cyclic voltammetry is small at a scan rate of 5 mV s^{-1}, demonstrating the great redox reversibility.

The electrochemical behavior of PB electrode in PVA gel electrolyte was investigated by cyclic voltammetry in a parallel configuration and the data are shown in Fig. 3C. PB exhibits well-defined redox pair of Prussian white (PW)/PB at 0.18 and 0.21 V in PVA gel electrolyte, similar to that obtained in PBS (0.1 M, pH = 6.0), demonstrating that there is no obvious influence of PVA gel on the K^+ diffusion in and out of the PB lattices. PVA gel electrolyte can thus be used to support the redox reaction of PB and consequently allow PB to make an electrochromic

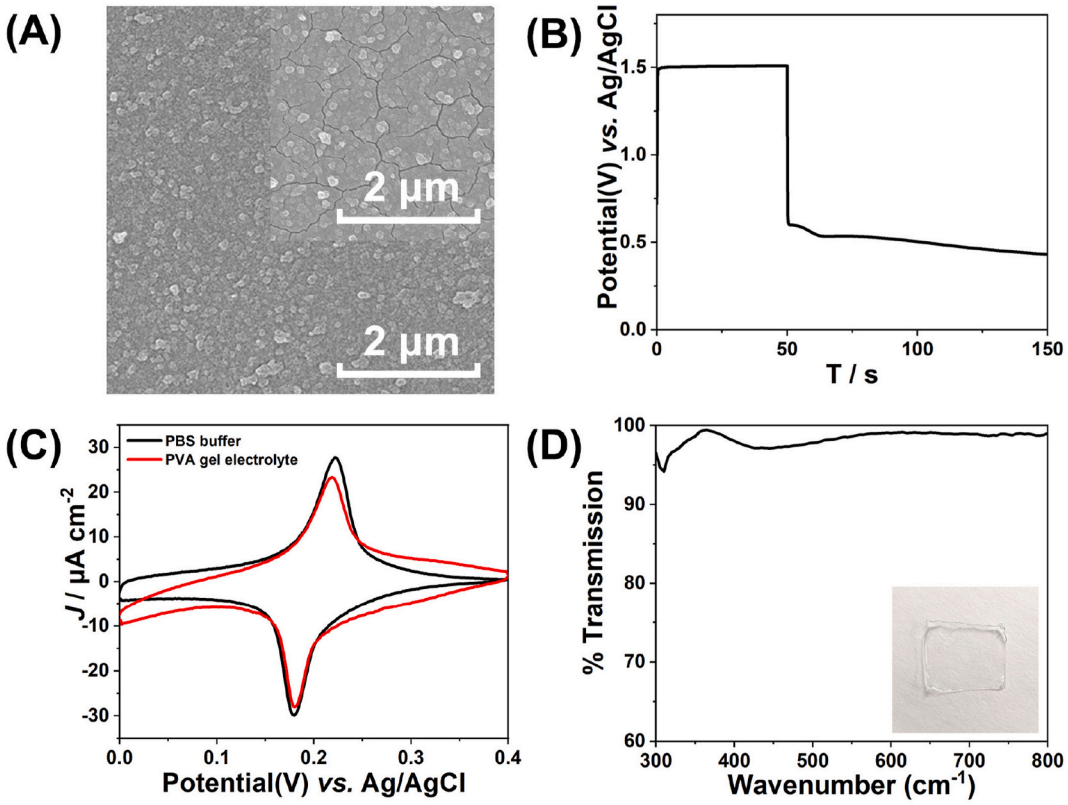

Fig. 3. (A) SEM image of a PB cathode after electrochemical activation, the inset is the image of the PB before activation. (B) Polarization curve for PB deposition with a deposition time of 100 s. (C) Cyclic voltammograms obtained with a PB cathode in PVA gel electrolyte (red) and PBS electrolyte (pH = 6.0, black), respectively, at a scan rate of 1 mV s^{-1}. (D) Transmission spectrum of PVA gel electrolyte in UV–visible region and a photograph of the PVA gel electrolyte. (For interpretation of the references to color in this figure legend, the reader is referred to the Web version of this article.)

response to the variation of the potential applied on it. The reasons for using PVA gel as a solid electrolyte in the sensor design also include that, (1) it can be prepared easily through a cross-linking method and a homogeneously thin gel electrolyte membrane can be formed by means of drop-casting due to its rheology property. The color change of PB overlaid by the thin PVA gel electrolyte membrane can be observed directly, as the latter offers a light transmission of over 90% in visible region, that is, it is transparent to visible light (Fig. 3D). (2) It has neither the redox activity in working potential nor the chemical reaction with formaldehyde, as a result, no interference to sensing performance resulted from it can be expected (Fan et al., 2014; Kobayashi et al., 1992). (3) Lateral ionic conductance of the PVA gel membrane can be adjusted effectively by varying the membrane thickness. Here the prepared PVA gel electrolyte exhibits a conductivity of 0.56 S cm^{-1} ± 0.08 S cm^{-1} (Fig. S6). (4) Since PB is not stable in neutral and especially basic media (Wang et al., 2009), it can benefit the stability of PB cathode by providing a weakly acidic environment originated from the phosphoric acid added for the cross-linking reaction. (5) It can promote the portability of the SPEB.

3.3. Characterization and performance of the naked-eye readout SPEB

The naked-eye readout SPEB towards gaseous formaldehyde can be obtained by confining a FDH/PMG/BP bioanode and a PB cathode horizontally on a patterned ITO substrate. When exposing to gaseous formaldehyde, the PB cathodes, act as the electrochromic displays, could accept electrons from the bioanodes and change the color from blue to colorless spontaneously, as the potential for PB reduction is obviously higher than that for formaldehyde oxidation at the bioanode (Sun et al., 2019). Due to the large lateral resistance of the PVA gel electrolyte membrane, the internal *iR* drop of the SPEB would become remarkable and lead to obvious potential gradient distribution on the PB cathode surface once the concentration of gaseous formaldehyde exceeding a critical value, and in this case, the discoloration of the PB cathode would occur progressively rather than homogeneously (Aller Pellitero et al. 2018, 2020). Therefore, according to the manner of color change, sensing information of the SPEB with a planar configuration can be extracted by analyzing the change in the color or the color patterns of the PB cathodes. It can be noticed that the pattern of PB on the cathode has two separated parts, one is a skull (part 1) and used to display sensing information when sensing low-level gaseous formaldehyde, and the other is a belt with two skulls (part 2) at the region far away from the bioanode compared to the part 1. The part 2 can be used as the reference or the display for low- or high-level gaseous formaldehyde determination, respectively.

PB cathodes with different PB deposition times have been prepared and used for the study on the influence of PB deposition time on the electrochromic properties of the PB cathodes that are related to sensing information display. The color of PB changes obviously from light blue to dark blue when prolonging the deposition time from 80 to 100 s, accordingly, an enhanced color contrast can be expected after PB reduction in the case of 100-s PB deposition time. No remarkable change in the color contrast can be observed by further extending the deposition time to 120 s (Fig. 4A and B). As the color image of PB cathode could be divided digitally into three independent channels, red (R), green (G), and blue (B), the ratio B/(R + G + B) that represents the intensity ratio of B channel to the referential RGB channels is considered as a standardized parameter to demonstrate the shade of blue color (Koh et al., 2016; Schreml et al., 2011). As shown in Fig. 4C, the average values of B/(R + G + B) obtained at the PB deposition time of 80, 100, and 120 s are 0.365, 0.385, and 0.387, and change to 0.337, 0.344, and 0.354 after reduction to PW, respectively. The changes in the RGB values demonstrate that the color contrast between PB and PW can be strongly enhanced by increasing the deposition time from 80 to 100 s, but no further obvious enhancement can be obtained by prolonging the deposition time to 120 s. When exposing to 400 ppb gaseous formaldehyde, the progressive discoloration of PB occurs and the skulls of part 1 at all three PB cathodes are discolored completely after 10 min. The discoloration of part l PB belt can also be observed at the cathode with a PB deposition time of 80 s, indicating the shorter PB deposition time leads to the requirement of PB films with the bigger length to balance the charge from the bioanode, which can be explained by the fact that the shorter PB deposition time results in the thinner PB films. Therefore, the performance of the PB cathode in displaying sensing information can be altered undoubtedly by varying the PB deposition time. Since high color contrast is an important concern in the design of optical, especially naked-eye readout with respect to the information extraction, the deposition time of 100 s is chosen for the fabrication of PB cathodes with enhanced color contrast, although it offers short discolored PB compared to the deposition time of 80 s.

The responses of the SPEBs to gaseous formaldehyde with different concentrations have been investigated and the images captured after 10-min exposure are shown in Fig. 5A. The positions of the color front estimated by the naked eye after treatment with a series of different concentrations of gaseous formaldehyde are shown in Fig. 5B, taking the front end of part 1 as the reference position. For 80 ppb gaseous formaldehyde, the color of the skull of part 1 at the cathode becomes slightly lighter and the color change is almost homogeneous, due to the negligible lateral *iR* drop resulted from the weak current, referred to the low level of gaseous formaldehyde. When increasing the concentration of gaseous formaldehyde, the progressive discoloration can be observed at the skull of part 1, and the color front moves away from the bioanode to balance the charge flowing in the circuit (Aller Pellitero et al., 2020). The skull of part 1 at the cathode is discolored completely as the concentration of gaseous formaldehyde increases to 400 ppb. The distance consumed after 10-min exposure is directly proportional to the gaseous formaldehyde concentration in a broad range of 80 and 400 ppb (inset of Fig. 5B), covering the values of several interesting indoor formaldehyde

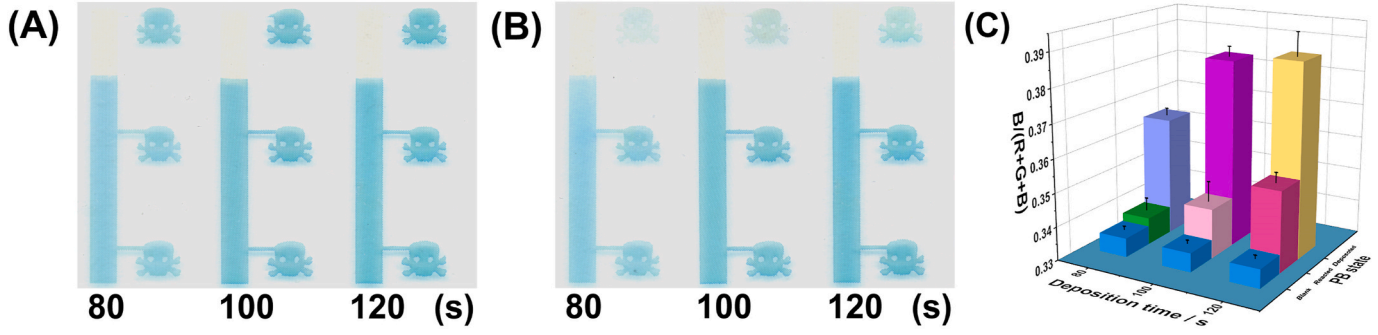

Fig. 4. (A) The images captured from the PB cathodes with different deposition time of 80 s, 100 s, and 120 s, respectively, arranged from left to right. (B) The images captured from the PB cathodes after 400 ppb formaldehyde treatment for 10 min. (C) B/(R + G + B) values obtained from the undeposited, reacted, and deposited PB cathodes, with different PB amounts. Error bars represented the standard deviations of 3 measurements.

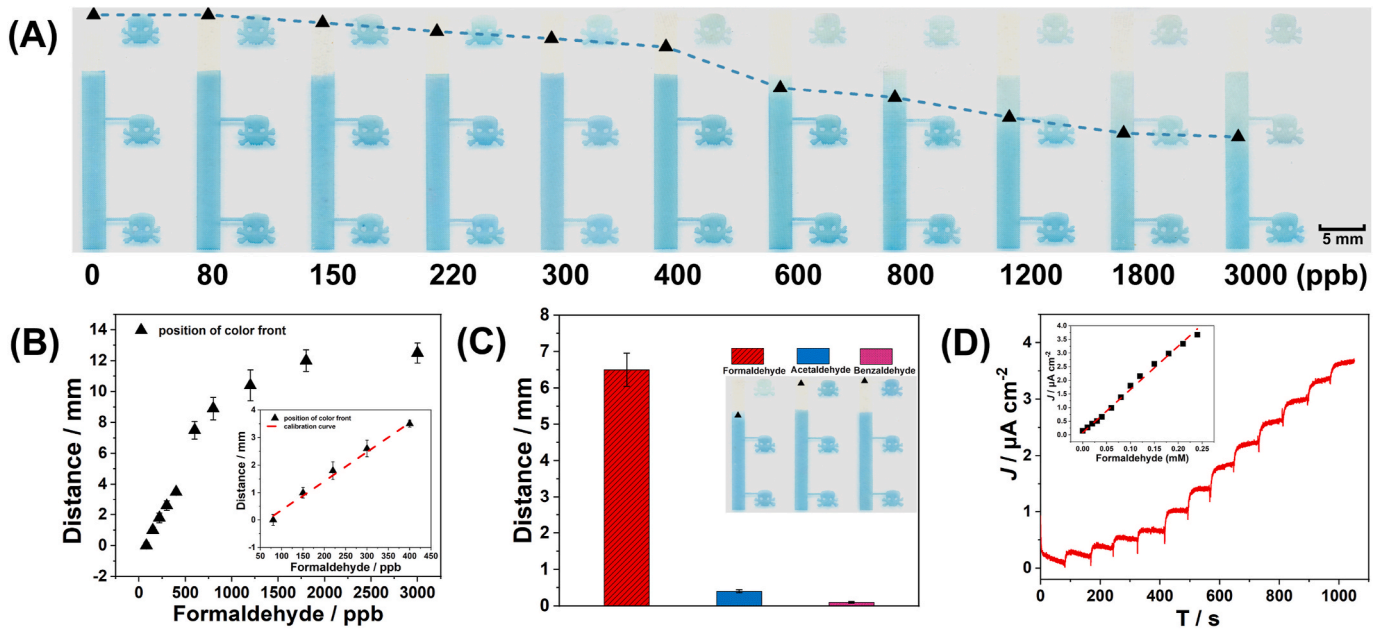

Fig. 5. (A) The images represent the evolution observed on PB cathodes after exposure to gaseous formaldehyde with the concentration from 0 to 3000 ppb for 10 min. Scale bar: 5 mm. (B) Discoloration distances obtained from PB cathodes as a function of the gaseous formaldehyde, inset: calibration curve of the naked-eye readout SPEB in the range of 80–400 ppb formaldehyde. (C) The images of the PB cathodes after exposure to 500 ppb formaldehyde, 500 ppb acetaldehyde, and 500 ppb benzaldehyde, from left to right, respectively. (D) Chronoamperometric response of the amperometric biosensor with successive additions of formaldehyde of known concentrations, recorded at 0 V, inset: calibration curve of formaldehyde concentration versus response current. The triangle points signaled the discoloration terminal of PB cathodes after 10-min exposure in formaldehyde. Error bars represented the standard deviations of 3 measurements.

exposure limits related to human health, for examples, 100 ppb for short-term exposure according to the guidelines of Canada (Murphy et al., 2013), and 300 ppb suggested to protect individuals against eye irradiation (Golden 2011).

The gaseous formaldehyde with concentrations higher than 400 ppb can further cause the progressive discoloration of the PB belt and skulls of part 2 after 10-min exposure, and the distance consumed increases with the concentration of gaseous formaldehyde up to 3000 ppb, but not linearly, mainly because the distribution of PB is not homogeneous along the potential gradient, due to the coupling of the PB belt and PB skulls. Despite the non-linear responses, the SPEB can be expected as a "Yes or No" type of sensor available in a broad gaseous formaldehyde concentration range up to 3000 ppb. By setting a threshold of the position of color front, the SPEB is able to make an alarm of formaldehyde exposure risk in some special indoor environments such as workplaces with a formaldehyde danger limit of 750 ppb (Castner et al., 2018). Given the fact that, for non-expert users of formaldehyde sensors, the goal of gaseous formaldehyde determination is to find the answer to the question that whether it is safe or not in certain indoor environments with respect to the formaldehyde exposure, that is, the level of formaldehyde is higher or lower than the suggested maximum exposure levels, but not to get the exact value of the concentration of indoor gaseous formaldehyde. Therefore, the SPEB could have good promise in indoor gaseous formaldehyde determination, given the characteristics such as the easy operation, the naked-eye readout, and the broad response range.

The selectivity of the naked-eye readout SPEB against two possible gaseous interferences has been investigated. As exhibited in Fig. 5C, no observable color change of the PB cathodes can be obtained in the presence of 500 ppb acetaldehyde or 500 ppb benzaldehyde, while obvious discoloration of the PB appears at the cathode under the same concentration of gaseous formaldehyde, indicating the excellent selectivity of the SPEB for formaldehyde detection. The high selectivity can be attributed to the specificity of FDH to formaldehyde. Besides, it is known that, the stability of enzymatic biosensors is predominantly determined by the enzymes used. Therefore, in order to evaluate the storage stability of the biosensor based on FDH, the FDH/PMG/BP bioanodes were prepared and stored at 4 °C, followed by assembling with PB cathodes when performed stability tests. The biosensors were treated with 400 ppb gaseous formaldehyde for 10 min and the images of PB cathodes were collected. As illustrated in Fig. S7A, the discoloration distance of PB cathode reduces along with storage period and could remain over 86% and 78% of its initial value after 10 and 14-day storages (Fig. S7B), which is comparable or superior to the biosensor based on FDH reported previously (Campbell and Rishpon 2001; Thanh-Thuy et al., 2014), suggesting the satisfactory storage stability.

The feasibility of the naked-eye readout SPEB in indoor formaldehyde determination is investigated by measuring the gaseous formaldehyde released from plywood, as decorated materials are believed to be the dominating sources of indoor gaseous formaldehyde. A container with a volume of 880 mL is used to collect the formaldehyde released from the plywood with a fixed surface area of 144 cm^2 in a time period of 50 min. Then, the naked eye readout SPEB is placed in the container and exhibits a distance of 3.2 ± 0.3 mm (n = 3) after 10 min (Fig. S8). According to the calibration curve shown in Fig. 5B, the concentration of the collected gaseous formaldehyde is thus determined to be 361 ppb. To check the accuracy of the result obtained with the naked-eye readout SPEB, the concentration of gaseous formaldehyde was also measured with the formaldehyde biosensor reported in our previous work (Sun et al., 2019). To get a liquid sample for the previously reported biosensor, a water glass containing 24 mL water is placed in the container to absorb the gaseous formaldehyde. According to the results of the naked-eye readout SPEB, the concentration of the liquid sample with a sampling time of 24 h should be 0.362 mg/L based on the assumption that the emission of the formaldehyde from the plywood is at a constant rate. The liquid sample is determined to be 0.340 ± 0.045 mg/L (n = 3) via the standard addition method by using the previously reported biosensor, as shown in Fig. 5D. The slight difference between the values of the formaldehyde concentrations determined with the naked-eye readout SPEB and the previously reported biosensor validate the feasibility and the accuracy of the naked-eye readout SPEB.

4. Conclusions

In summary, a portable, fast, reliable, layman-friendly, and naked-eye readout SPEB for on-site gaseous formaldehyde determination has been fabricated by integrating a planar FDH/PMG/BP bioanode and a planar PB cathode on a patterned ITO substrate. The progressive discoloration of PB at the cathode has been achieved based on the large lateral resistance of the PVA gel electrolyte. The color front moves far away from the bioanode with the increase of the gaseous formaldehyde concentration in a broad range of 80 and 3000 ppb with excellent anti-interference ability, and the distance consumed of the PB cathode after 10-min exposure is linearly dependent on the concentration of gaseous formaldehyde in the range of 80 and 400 ppb. The naked-eye readout SPEB has been used for practical applications and the satisfying result in sensing gaseous formaldehyde released from the real plywood is obtained. The excellent sensing performances, coupled with the advantages such as ease of operation, mass production capability, and portability, indicate great potential of the naked-eye readout SPEB as an economically viable device in living environmental protection and considerate individual health care. Moreover, the design of the proposed biosensor can be adopted as a general one to develop naked-eye readout SPEB biosensors toward other analytes, as FDH can be readily replaced by other enzymes.

CRediT authorship contribution statement

Xiaoxuan Sun: Conceptualization, Methodology, Investigation, Formal analysis, Writing - original draft. **He Zhang:** Methodology, Investigation, Validation. **Liang Huang:** Formal analysis, Resources. **Shuai Hao:** Visualization, Data curation. **Junfeng Zhai:** Conceptualization, Writing - review & editing, Supervision, Project administration. **Shaojun Dong:** Conceptualization, Writing - review & editing, Supervision, Project administration, Funding acquisition.

Declaration of competing interest

The authors declare that they have no known competing financial interests or personal relationships that could have appeared to influence the work reported in this paper.

Acknowledgments

This work was supported by the National Natural Science Foundation of China (no. 21721003 and 21675151) and the Ministry of Science and Technology of China (no. 2016YFA0203203).

Appendix A. Supplementary data

Supplementary data to this article can be found online at https://doi.org/10.1016/j.bios.2021.112975.

References

Achmann, S., Hämmerle, M., Moos, R., 2008a. Electroanalysis 20 (4), 410–417.
Achmann, S., Hermann, M., Hilbrig, F., Jérôme, V., Hämmerle, M., Freitag, R., Moos, R., 2008b. Talanta 75 (3), 786–791.
Aller Pellitero, M., Santiago-Malagón, S., Ruiz, J., Alonso, Y., Lakard, B., Hihn, J.-Y., Guirado, G., del Campo, F.J., 2020. Sens. Actuators, B 306, 127535.
Aller Pellitero, M., Guimera, A., Kitsara, M., Villa, R., Rubio, C., Lakard, B., Doche, M.-L., Hihn, J.-Y., Javier del Campo, F., 2017. Chem. Sci. 8 (3), 1995–2002.
Aller Pellitero, M., Guimera, A., Villa, R., Javier del Campo, F., 2018. J. Phys. Chem. C 122 (5), 2596–2607.
Campbell, C.E., Rishpon, J., 2001. Electroanalysis 13 (1), 17–20.
Castner, J., Gehrke, G.E., Shapiro, N., Dannemiller, K.C., 2018. Publ. Health Nurs. 35 (4), 261–272.
Celiesiute, R., Ramanaviciene, A., Gicevicius, M., Ramanavicius, A., 2019. Crit. Rev. Anal. Chem. 49 (3), 195–208.
Chung, P.-R., Tzeng, C.-T., Ke, M.-T., Lee, C.-Y., 2013. Sensors 13 (4), 4468–4484.
Coleman, B., Coarsey, C., Asghar, W., 2019. Analyst 144 (6), 1935–1947.
Demkiv, O., Smutok, O., Paryzhak, S., Gayda, G., Sultanov, Y., Guschin, D., Shkil, H., Schuhmann, W., Gonchar, M., 2008. Talanta 76 (4), 837–846.
Dong, C., Wang, Z., Zhang, Y., Ma, X., Iqbal, M.Z., Miao, L., Zhou, Z., Shen, Z., Wu, A., 2017. ACS Sens. 2 (8), 1152–1159.
Dong, S., Dasgupta, P.K., 1986. Environ. Sci. Technol. 20 (6), 637–640.
Fan, L.-Q., Zhong, J., Wu, J.-H., Lin, J.-M., Huang, Y.-F., 2014. J. Mater. Chem. 2 (24), 9011–9014.
Fu, J., Zhang, L., 2018. Anal. Chem. 90 (13), 8080–8085.
Fu, L., Liu, J., Hu, Z., Zhou, M., 2018. Electroanalysis 30 (11), 2535–2550.
Gai, P., Gu, C., Hou, T., Li, F., 2017. Anal. Chem. 89 (3), 2163–2169.
Golden, R., 2011. Crit. Rev. Toxicol. 41 (8), 672–721.
Gross, A.J., Holzinger, M., Cosnier, S., 2018. Energy Environ. Sci. 11 (7), 1670–1687.
Hämmerle, M., Hall, E.A., Cade, N., Hodgins, D., 1996. Biosens. Bioelectron. 11 (3), 239–246.
Hao, S., Sun, X., Zhang, H., Zhai, J., Dong, S., 2020. J. Mater. Chem. B 8 (16), 3393–3407.
Hou, C., Fan, S., Lang, Q., Liu, A., 2015. Anal. Chem. 87 (6), 3382–3387.
Itaya, K., Uchida, I., 1986. Inorg. Chem. 25 (3), 389–392.
Kobayashi, H., Ikada, Y., Moritera, T., Ogura, Y., Honda, Y., 1992. J. Biomed. Mater. Res. 26 (12), 1583–1598.
Koh, A., Kang, D., Xue, Y., Lee, S., Pielak, R.M., Kim, J., Hwang, T., Min, S., Banks, A., Bastien, P., Manco, M.C., Wang, L., Ammann, K.R., Jang, K.-I., Won, P., Han, S., Ghaffari, R., Paik, U., Slepian, M.J., Balooch, G., Huang, Y., Rogers, J.A., 2016. Sci. Transl. Med. 8 (366).
Liana, D.D., Raguse, B., Gooding, J.J., Chow, E., 2015. ACS Appl. Mater. Interfaces 7 (34), 19201–19209.
Lin, S., Li, D., Wu, J., Li, X., Akbar, S.A., 2011. Sens. Actuators, B 156 (2), 505–509.
Maddalena, R., Russell, M., Sullivan, D.P., Apte, M.G., 2009. Environ. Sci. Technol. 43 (15), 5626–5632.
Murphy, M.W., Lando, J.F., Kieszak, S.M., Sutter, M.E., Noonan, G.P., Brunkard, J.M., McGeehin, M.A., 2013. Indoor Air 23 (2), 134–141.
Narváez Villarrubia, C.W., Rincón, R.A., Radhakrishnan, V.K., Davis, V., Atanassov, P., 2011. ACS Appl. Mater. Interfaces 3 (7), 2402–2409.
Roche, J., Groenen-Serrano, K., Reynes, O., Chauvet, F., Tzedakis, T., 2014. Chem. Eng. J. 239, 216–225.
Salthammer, T., Mentese, S., Marutzky, R., 2010. Chem. Rev. 110 (4), 2536–2572.
Schreml, S., Meier, R.J., Wolfbeis, O.S., Landthaler, M., Szeimies, R.-M., Babilas, P., 2011. Proc. Natl. Acad. Sci. U. S. A. 108 (6), 2432–2437.
Sun, X., Zhang, H., Hao, S., Zhai, J., Dong, S., 2019. ACS Sens. 4 (10), 2631–2637.
Suzuki, Y., Nakano, N., Suzuki, K., 2003. Environ. Sci. Technol. 37 (24), 5695–5700.
Tang, X., Bai, Y., Duong, A., Smith, M.T., Li, L., Zhang, L., 2009. Environ. Int. 35 (8), 1210–1224.
Thanh-Thuy, N.-B., Saulnier, J., Jaffrezic-Renault, N., Lagarde, F., 2014. Anal. Bioanal. Chem. 406 (4), 1039–1048.
Wang, X., Gu, H., Yin, F., Tu, Y., 2009. Biosens. Bioelectron. 24 (5), 1527–1530.
Wei, W., Guo, S., Chen, C., Sun, L., Chen, Y., Guo, W., Ruan, S., 2017. J. Alloys Compd. 695, 1122–1127.
Wen, D., Deng, L., Guo, S., Dong, S., 2011. Anal. Chem. 83 (10), 3968–3972.
Yang, P., Sun, P., Mai, W., 2016. Mater. Today 19 (7), 394–402.
Zhang, X., Zhang, L., Zhai, Q., Gu, W., Li, J., Wang, E., 2016. Anal. Chem. 88 (5), 2543–2547.
Zhou, M., 2015. Electroanalysis 27 (8), 1786–1810.
Zhou, X.L., Mopper, K., 1990. Environ. Sci. Technol. 24 (12), 1864–1869.
Zloczewska, A., Celebanska, A., Szot, K., Tomaszewska, D., Opallo, M., Joensson-Niedziolka, M., 2014. Biosens. Bioelectron. 54, 455–461.